# X-RAY LINE BROADENING FROM FILED ALUMINIUM AND WOLFRAM*

## G. K. WILLIAMSON† and W. H. HALL†

Methods of analysis previously used in the interpretation of line broadening are discussed and are shown to be inadequate; more reliable methods being outlined. An analysis of published results using one of these methods suggests that the observed effects can be attributed to simultaneous small particle size and strain broadening. Measurements of the changes in intensity distribution have been made, using a Geiger counter spectrometer, in the spectra of cold worked aluminium and wolfram. The line breadths may be attributed to simultaneous small particle size and strain broadening, the latter predominating, particularly at the higher Bragg angles, and it is shown that the observed effects are produced by dislocations or some similar structural fault. The observed rise in the breadths of the high angle lines from annealed materials suggests that some dislocations remain after annealing. Fourier analysis of the line shapes in general merely confirm the results of the analysis of the line breadths, but in the case of the recovered specimens it suggests that the dislocations form into walls ("polygonization").

## L'ELARGISSEMENT DES RAIES DE RAYONS X OBTENUES DES LIMAILLES D'ALUMINIUM ET DE TUNGSTENE

Les méthodes utilisées auparavant dans l'interprétation de l'élargissement des raies sont discutées et il est montré qu'elles sont inadéquates; des méthodes plus correctes sont indiquées. L'examen des résultats publiés, obtenus au moyen d'une des ces méthodes, fait croire que les effets observés peuvent être attribués en même temps à la petitesse des particules et à l'élargissement dû à la déformation. Les variations de la distribution d'intensité dans les spectres d'aluminium et de tungstène ont été mesurées au moyen d'un spectromètre à compteur Geiger. Les largeurs des raies peuvent être attribuées simultanément à la petitesse des particules et à l'élargissement dû à la déformation, cette dernière étant la plus importante, surtout aux plus grands angles de Bragg, il est aussi démontré que les effets observés sont dûs aux dislocations ou à un autre défaut structural, similaire. L'augmentation observée dans la largeur des raies à grand angle obtenues des matériaux recuits, fait croire, qu'une partie des dislocations reste après recuit. L'analyse de Fourier de la forme des raies confirme en général les résultats d'analyse de la largeur des raies, mais dans le cas des échantillons qui ont subi un recuit de restauration, cela conduit plutôt à la conclusion que les dislocations se rangent en plans (polygonisation).

## DIE VERBREITERUNG DER ROENTGENINTERFERENZLINIEN VON ALUMINIUM- UND WOLFRAMSPAENEN

Die analytischen Methoden, die bisher zur Auswertung von Messungen der Linienverbreiterung von Röntgeninterferenzen benutzt wurden, werden diskutiert. Es wird gezeigt, dass sie unzureichend sind, und zuverlässige Methoden werden beschrieben. Analysiert man die in der Literatur veröffentlichten Daten nach einer dieser Methoden, so scheint die beobachtete Verbreiterung sowohl auf den Effekt der kleinen Teilchengrösse als auch auf innere Spannungen zurück zu gehen. Veränderungen in der Intensitätsverteilung der Feinstrukturdiagramme von kaltbearbeitetem Aluminium und Wolfram wurden mit Hilfe eines Zählrohr-Spektronometers gemessen. Die Linienverbreiterung kann auf die gleichzeitig vorhandenen Effekte kleiner Teilchengrösse und innerer Spannungen zurückgeführt werden; der Einfluss der Spannungen überwiegt, vor allem bei grossen Reflexionswinkeln. Es wird gezeigt, dass die beobachteten Effekte durch Versetzungen ("dislocations") oder ähnliche Kristallbaufehler hervorgerufen werden. Die beobachtete Verbreiterung der Linien grosser Reflexionswinkel in geglühten Materialien deutet darauf hin, dass nach der Glühung noch einige Versetzungen ("dislocations") im Material zurückbleiben. Fourieranalyse der allgemeinen Linienform bestätigt nur die Resultate der Analyse der Linienverbreiterung. Allein bei erholten Proben deutet sie darauf hin, dass sich die Versetzungen ("dislocations") zu Wänden zusammenschliessen ("Polygonisation").

## Introduction

The cold working or plastic deformation of metals has been shown to produce appreciable changes in the intensity distribution of diffracted X-rays. The most prominent of these effects are changes in line shape and in integrated intensity, and previous workers have usually confined their studies to one or other of these topics. Changes in integrated intensity have been studied and discussed by Hall and Williamson [1] and it is the object of this paper to interpret, discuss and correlate the changes in line shape with the simultaneous measurements of integrated intensity reported previously.

Previous work suggests that the broadening is produced by either lattice strains alone, or by lattice strains and small particle size simultaneously. Stokes and Wilson [2] have shown that if the integral breadth of the strain distribution is $\xi$ the corresponding spectral integral line breadth‡ $\beta_s$ due to strains is

$$(1) \qquad \beta_s = 2\xi \tan \theta$$

where $\theta$ is the Bragg angle, a relation deduced by many earlier workers. In terms of the reciprocal lattice the effect of lattice strain is to broaden the reciprocal lattice points to a breadth $\beta_s^*$ which varies linearly with the distance from the origin,

‡Spectral breadths are usually measured in terms of the dispersion $\chi$ (a scale of $2\theta$).

$d^*$, thus, since $\beta^* = \beta \cos \theta / \lambda$ and $d^* = 2 \sin \theta / \lambda$

$$\beta_s^* = \xi d^* \tag{2}$$

(Lipson [3]).

Particle size broadening has been shown by many investigators to obey the relation

$$\beta_P = \lambda / t \cos \theta \tag{3}$$

where $\lambda$ is the X-ray wavelength, and $t$ is a mean linear dimension of the particle defined by Stokes and Wilson [2], and has been called the apparent particle size by Jones [4]. The reciprocal lattice breadth $\beta_P^*$ is a constant independent of $d^*$ and equal to $1/t$.

Correction for experimental broadening necessarily introduced by imperfections of the camera and recording device have been discussed in detail by Jones [4]. Stokes and Wilson [2], Schull [5] and Stokes [6] have suggested and described Fourier methods of correction which require no *a priori* assumptions of experimental and broadening function line shapes.

## Previous Work

Since the first report of line broadening by van Arkel [7] most of the published work has been held to support the view that broadening is due to randomly directed, slowly varying internal lattice strains. Wood [8; 9], Haworth [10], Brindley and Ridley [11], Brindley [12], Smith and Stickley [13], Stokes, Pascoe and Lipson [14], Megaw and Stokes [15] have used similar methods of interpretation in supporting the "strain" hypothesis. For example, Smith and Stickley [13] found that the physical broadening (i.e. the measured breadth corrected for experimental broadening) from wolfram was linear with tan $\theta$ (equation (1) for lattice strain effects) showing no dependence on wavelength (equation (3) for particle size broadening). The same results plotted against sec $\theta$ (equation (3)) indicated a negative value of $\beta$ when $\lambda$ sec $\theta$ was zero, a physically meaningless result.

For $\alpha$-brass Smith and Stickley were able to resolve the variation in the apparent strain $2\xi$ with the indices of reflection in terms of the elastic anisotropy of brass. They suggested that $\xi/2$ should have an order of magnitude $U/E$, where $U$ is the tensile strength and $E$ Young's modulus, and found good agreement between these two values.

Further evidence in favour of the lattice strain theory, differing in the method of interpretation from the above, is that advanced by Warren and Averbach [16; 17]. They studied the changes in line

shape rather than changes in line breadth and concluded that line broadening is due to lattice strains, which are not constant over distances greater than about 10 atomic diameters.

Evidence supporting the contention that some of the broadening is due to particle size is generally less convincing. Dehlinger and Kochendörfer [18] attempted some separation between particle size and strain effects by attributing the low angle broadening to small particle size. Bragg [19; 20] related the strength of metals to their apparent particle size and found good agreement between the observed values and those calculated from the data of Wood [21; 22], and Wood and Rachinger [23] have reported some dependence of the observed broadening upon wavelength, in agreement with equation (3).

## Discussion of the Theories of Line Broadening

Any complete theory of line broadening must relate the cause of line broadening to the existing theories of work-hardening and plastic deformation, explain the apparent anomalies between the two conflicting interpretations just reviewed, and relate the line broadening to the changes in integrated intensity produced by cold work.

One useful approach is to consider a spectrum in which both strain and small particle size broadening occur simultaneously, to calculate the variation of the total broadening $\beta$ with $\theta$, and to apply the tan $\theta$ and sec $\theta$ criteria as used by previous workers supporting the strain hypothesis. In Figure 1, the
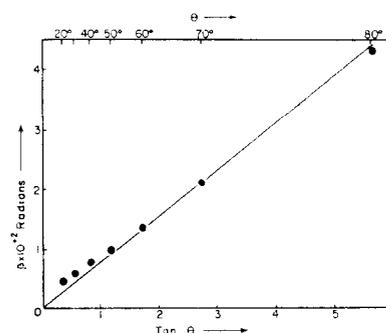


FIGURE 1. A plot of the physical broadening $\beta$ due to simultaneous small particle size and strain broadening against tan $\theta$. The calculated points correspond closely to a straight line through the origin despite the presence of appreciable particle size broadening.

values of $\beta$ calculated for typical values of $t/\lambda = 250$, $2\xi = 0.5$ per cent, and on the assumption that the breadths are additive is plotted against tan $\theta$. The plot is linear within a small margin of error, the greatest discrepancy being apparent below $\theta = \chi/2 = 30°$ where experimental accuracy is usually low. The plot of $\beta$ against sec $\theta$ (Figure 2) shows that the
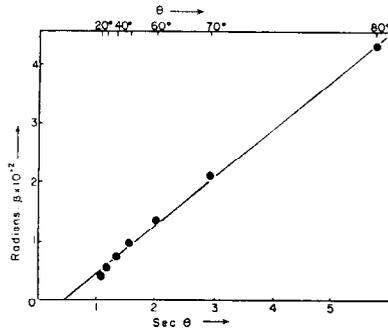
FIGURE 2. A plot of the physical broadening $\beta$ due to simultaneous small particle size and strain broadening against sec $\theta$. Any reasonable line through the calculated points gives a negative intercept.

high angle points correspond fairly closely to a straight line having a negative intercept at sec $\theta = 0$. Thus Figures 1 and 2 correspond closely to those previously reported experimental results which have been held to support the strain theory, although they have been calculated on the assumption that appreciable small particle size broadening exists in the spectrum; the tan $\theta$ and sec $\theta$ plots cannot therefore be regarded as satisfactory criteria in the interpretation of line broadening.

The interpretation of results obtained with many wavelengths may also be misleading since $\theta$ and $\lambda$ are not independent variables.

In general $\beta$ is given approximately by

(4)          $\beta = 2\xi \tan \theta + \lambda/t \cos \theta$,

and on substituting from the Bragg Law for $\lambda$ then

(5)          $\beta = (2\xi + 2d/t) \tan \theta$

and the breadth is a linear function of tan $\theta$ for any one reflection (hkl) irrespective of the nature of the broadening (the values of $2\xi$ and $2d/t$ are dependent on the indices of reflection). This too is in agreement with the reported work (e.g. Brindley and Ridley, Smith and Stickley).

The interpretation in terms of small particle effects has been criticized by Stokes, Pascoe and Lipson [14] and by Stokes and Lipson [24] and also appears to be in doubt.

Hall [25] proposed a method of interpretation allowing some separation of particle size broadening and strain broadening. The method consists essentially in plotting the breadth of the reciprocal lattice points against their distance from the origin. Small particle size alone then gives a horizontal plot with an intercept $1/t$, and strain gives a line through the origin slope, $\xi$, if the strain distribution is isotropic.

The composite broadening produced by simultaneous small particle size and strain depends to some

extent on the broadening functions of the separate effects. If both broadening functions are Cauchy curves (of the form $1/(1 + k^2 x^2)$) then the breadths are additive and the plot is linear with slope $\xi$ and intercept $1/t$ (curve a, Fig. 3). If the broadening
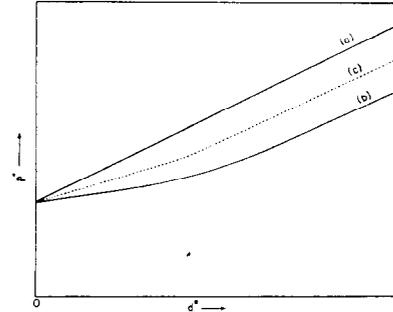


FIGURE 3. A plot of $\beta^*$ ( $= \beta \cos \theta/\lambda$) due to simultaneous small particle size and strain broadening against $d^*$ ( $= 2 \sin \theta/\lambda$). Curve (a) is obtained if the broadening functions are of the Cauchy type whilst curve (b) is that obtained if the functions are Gaussians. The dotted curve (c) represents an intermediate case discussed in the text.

functions are Gaussians, the squares of the breadths are additive and the graph is curved, being asymptotic to a line of slope $\xi$ curving upwards near the origin to an intercept $1/t$, (curve b, Fig. 3). Since the curvature is dependent on the exact forms of the line shapes and broadening functions assumed, it is preferable to calculate the type of variation expected from various models. Such a calculation for a randomly strained crystal is discussed below, and it is of interest to note that Wilson [26] has generalised his calculation on diffraction by bent lammelae to show that there is a similar gradual transition from pure particle size broadening at $d^* = 0$ to strain broadening for large values of $d^*$.

Warren and Averbach [17] have shown that the strains and particle size of a sample can be deduced from the Fourier coefficients $A_n$ of the broadening function and the breadth of the reciprocal lattice broadening function is given by

(6)          $\beta^* = a_3^* \Big/ \sum_{-\infty}^{+\infty} A_n$

It follows that it is possible to obtain the variation of the breadth throughout the reciprocal lattice by calculating the Fourier coefficients for a particular model. It is convenient to obtain Warren and Averbach's $A_n$ by folding the coefficients due to particle size $P_n$ with the corresponding coefficients due to internal strains, $S_n$. By choosing new axes any reflection can be made the ool reflection from planes of fundamental spacing $a_3$. If cells along columns perpendicular to the reflecting plane suffer displace-

ments which have a Gaussian distribution such that the mean square displacement for cells $na_3$ apart is $\langle Z_n^2 \rangle_{av.}$, then

$$(7) \qquad S_n = \exp(-2\pi^2 l^2 \langle Z_n^2 \rangle_{av.})$$

(Warren and Averbach, [17, equation 14]).

The term $P_n$ is the ratio of the number of cells $n$ spacings apart to the total number of cells, and thus for a crystal of length $N_3$ perpendicular to the reflecting planes

$$(8) \qquad P_n = (N_3 - n)/N_3.$$

Thus the coefficient $A_n$ due to both small particle size and internal strains is

$$(9) \qquad A_n = (1 - n/N_3)\exp(-2\pi^2 l^2 \langle Z_n^2 \rangle_{av.})$$

Quite generalized arguments show that as $l$ approaches zero the strain component approaches unity and the breadth approaches pure particle size broadening

$$(10) \qquad \beta^* \rightarrow \left( a_3 \sum_{-N_3}^{+N_3} 1 - n/N_3 \right)^{-1} = \frac{1}{t}.$$

At large values of $l$, $P_n$ becomes virtually constant compared to the rapid variation in $S_n$ and the high angle broadening approximates to pure strain broadening. More particularly, if the strain varies slowly within the crystal then $\langle Z_n^2 \rangle_{av.} = n^2 \bar{\eta}^2$ where $\bar{\eta}^2$ is the mean square strain and, when $l^2 \bar{\eta}^2$ is small,

$$(11) \qquad A_n \simeq (1 - n/N_3)(1 - 2\pi^2 l^2 \bar{\eta}^2 n^2)$$

whence

$$(12) \qquad \sum A_n \simeq N_3(1 - \pi^2 l^2 \bar{\eta}^2/3)$$

and

$$(13) \qquad \beta^* \simeq 1/t(1 - \pi^2 l^2 \bar{\eta}^2/3).$$

Hence to the extent that the approximation holds the plot of $\beta^*$ against $d^*$ (which equals $la_3^*$) intersects $d^* = 0$ at $1/t$ and curves away from the horizontal line representing particle size very rapidly with increasing $d^*$.

For a crystal in which $l^2 \bar{\eta}^2$ is large,

$$(14) \qquad \sum A_n = (1/l\sqrt{2\pi\bar{\eta}^2}) - (1/N_3 2\pi^2 l^2 \bar{\eta}^2)$$

and

$$(15) \qquad \beta^* \sim (d^*\sqrt{2\pi\bar{\eta}^2}) + (1/\pi t).$$

Thus for large values of $\bar{\eta}^2$ or $d^*$ this approximates to $\beta^* = d^* \sqrt{(2\pi\bar{\eta}^2)}$ i.e. $\beta_x = 2 \sqrt{(2\pi\bar{\eta}^2)} \tan \theta$ which may be compared with equation (1) for strain broadening in which $\xi = \sqrt{(2\pi\bar{\eta}^2)}$. This result coincides with curve b, Figure 3, deduced by a more

qualitative discussion. The strain distribution appears to lie between the two extremes of Cauchy and Gaussian functions and a general curve such as Figure 3c is probable. The use of a linear extrapolation from measurements at high angles only, results in correct values of the lattice strain for all cases but values of particle size which may be too large by a factor in the range 1 to $\pi$.

Hall [25] analysed much of the published data using a plot of $\beta^*$ against $d^*/2$ using a linear extrapolation and found a positive intercept for all cases excepting that of martensite, the particle sizes ranging about a value of $10^{-5}$cm. A similar value has also been reported by Mazur [27] and by Krainer [28] for martensite. The slopes (and hence the mean strains) increased generally with the hardness of the metals.

An interpretation attributing broadening to simultaneous particle size and strain effects seems to correlate most of the published results, and, as will be shown later, this is in good accord with the current dislocation theory of deformation. Since the method used by Hall involves a long extrapolation from the experimental points further measurements have been made using an improved experimental technique in order that a more certain correlation of the observed effects with the dislocation theory can be made.

Aluminium and wolfram have been chosen for study, since they are both approximately elastically isotropic. These two metals also approximate to the extremes of hardness normally encountered in metals, aluminium being one of the softest metals and wolfram one of the hardest, and it may be possible to determine the influence of hardness on the changes observed.

## Preparation of Specimens

All specimens used in these experiments were prepared by hand filing, followed by sieving through a 350 mesh per inch sieve.

Four samples of aluminium were prepared, two from a sample of high purity aluminium greater than 99.99 per cent pure, and two from a sample of commercially pure aluminium (approximately 99.7 per cent Al), using a "smooth" file. Filings of both purities annealed in vacuo (less than $10^{-2}$ cm. mercury) at 500°C for 25 minutes, but as the line breadths from both were found to be identical only the spectrum of the high purity sample was examined in detail.

Three specimens of wolfram were prepared from a bar 99.9 per cent pure supplied by the Tungsten

Manufacturing Co. After sieving, the filings were shown by analysis to contain less than 0.4 per cent of iron. Two samples were annealed in vacuo, one for 50 minutes at 1150°C and the other for 3 hours at 1300°C.

## The Experimental Method

The results were obtained using a Geiger counter spectrometer and the experimental methods previously described [1], the measurements of line shape being carried out simultaneously with those of the changes in intensity previously reported. Measurements were made of the reflected intensity, using a scaling unit, at specific angular settings of the Geiger counter in order to avoid the distortion introduced by the use of a counting-rate meter [29]. The "count" was recorded on the scaling unit, not for a constant time, but for an arbitrary monochromatic X-ray output from the X-ray set as measured on a second monitoring counter and was corrected for counting losses (Hall and Williamson [30]). Frequent checks on the stability of the monitoring were made and although a long term drift of ± 2 per cent was observed, the drift of less than 1 per cent during the measurement of any one line would introduce a distortion less than uncertainty due to statistical scatter on the results; monochromatized copper $K_\alpha$ radiation generated at 50 K.V. peak and 10 M.A. has been used throughout.

Integral line breadths were obtained by graphical resolution of the line shapes [31] to obtain the sum of the $\alpha_1$ and $\alpha_2$ peak intensities, Simpson's rule being used to determine the integrated intensity. The resolved line shapes coincided with Cauchy functions within experimental error and thus the observed breadth is simply the sum of the required physical breadth and the experimental breadth.

## Line Broadening Results for Aluminium

The values of the line breadths observed in the spectra from the three aluminium specimens are shown in Figure 4 in which $N = h^2 + k^2 + l^2$ and the breadth $B_\chi$ is expressed in minutes of arc in $\chi$. Two features are noticeable: first, the very low value of the broadening in the cold worked, high purity specimen compared to that in the commercially pure specimen, and secondly, the rapid rise in the broadening at high angles in the annealed specimen. This latter effect is due to physical broadening, since Alexander [32] has shown that the form of the experimental broadening is that shown dotted in Figure 4. Particle sizes as small as $5 \times 10^{-5}$ cm. are inadequate to explain this broadening and it appears that lattice strains exist even in the annealed state.
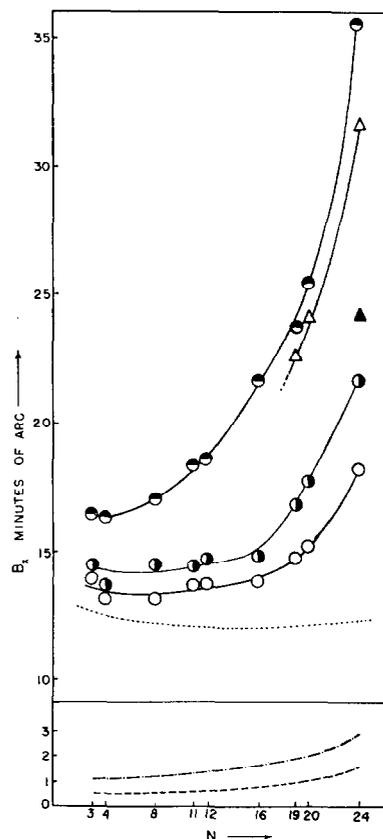


FIGURE 4. The line breadths $\beta_\chi$ for the aluminium spectra plotted against $N = h^2 + k^2 + l^2$. O from the high purity annealed sample; ◑ from the high purity filed sample; ● from the commercial purity filed sample; △ from the slowly mechanically filed high purity sample; ▲ from the high purity samples rapidly filed under liquid air; ...... the predicted form of the experimental broadening; — — — — physical broadening produced by a particle size of $10^{-4}$ cm; •—•—•—• physical broadening produced by a particle size of $5 \times 10^{-5}$ cm.

An estimation of the experimental broadening must be made before the results can be interpreted, since no direct measure is possible. The divergence of the X-rays has been restricted to 2° and the experimental broadening is approximately symmetrical about $\chi = 90°$. A constant experimental breadth has therefore been chosen for two lines equidistant from $\chi = 90°$ (in Fig. 5, lines 3 and 24), such that the reciprocal lattice broadening indicates a particle size of $0.8 \times 10^{-4}$ cm. for the annealed state, a value which is of the correct order of magnitude [33]. Both cold worked specimens have smaller particle sizes a value of $4 \times 10^{-5}$ cm. being indicated for both purities on Figure 5.

The values of $\beta^*$ for the other lines, calculated for the same assumed experimental breadth of 12′, lie on a smooth curve and indicate the lack of anisotropy in the broadening. The assumption of symmetrical experimental broadening and Cauchy line shapes, tends to reduce the slope of the reciprocal
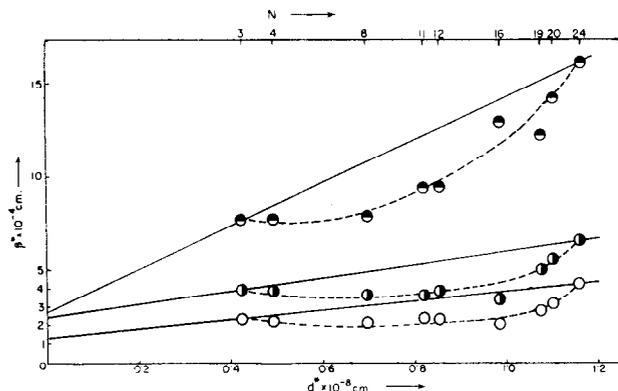
FIGURE 5. The interpretation of the line broadening in the aluminium spectra in which $\beta^*$ is plotted against $d^*$ assuming an experimental breadth of 12 mins. of arc. Symbols as for Figure 4.

lattice broadening so that the values of the lattice strain breadths of 0.025 per cent for annealed aluminium, 0.045 per cent for filed high purity, and 0.14 per cent for filed commercial purity are minimum and not absolute values.

The different impurity content of the two filed specimens is probably responsible for the differences in the strain breadths since both received the same cold working treatment, the impurities retarding or preventing the recovery of the commercial specimen. No difference in line broadening could be detected in the high purity sample examined $\frac{1}{2}$ hour, and 350 hours after filing and this suggests that the recovery, if any, occurred at the instantaneous high temperature generated during filing. Further high purity samples were examined in which this instantaneous temperature rise was restricted, either by filing very slowly with a lightly loaded file so that the heat generated was dissipated very rapidly, or by filing under liquid air. Both these methods gave increased broadening as shown in Figure 4, the slowly filed sample having a broadening little different from that of the commercially pure specimen, confirming that the difference is due to instantaneous recovery on filing.

## Discussion of Results for Aluminium

The effect of recovery on the value of the breadths is of great interest in view of the simultaneous measurements of the changes in integrated intensity and background level [1]. In these experiments cold work was observed to produce a uniform reduction in the intensities of each reflection (after a corrrection for extinction which is also affected by cold work) and a corresponding rise in the background level. The intensities of the lines and the background level were not affected by recovery, within the limits of

experimental accuracy. Since the background rise was substantially constant over the entire spectrum very large atomic displacements of the order of up to half a spacing must be responsible. These two results together provide a very critical test for any theory of cold work, since the very high short range strains responsible for the increase in background intensity and the decrease in line intensity must be more stable at the high temperature produced during filing than the small long range strains responsible for the increase in line breadths. The simple random lattice strain theory is inadequate for this reason since the greater the strain the less should be its stability; on recovery the background would be expected to change first, and not the line broadening as observed. The only satisfactory explanation is that some metastable fault exists which produces the high short range strains and persists even after the dissipation of the smaller long range strains.

Two types of lattice fault which would conform to the stringent requirements of the experimental data are the screw and edge dislocations, which are stable in so far as they can only be removed from the lattice by movements to a free boundary or by mutual annihilation of two dislocations of opposite sign. A detailed discussion of the dislocation theory is beyond the scope of this paper and excellent reviews exist (see for example Burgers [34], and Cottrell [35]).

From the dislocation models produced by Bragg and Nye [36] for a bubble raft, and by Bilby [37] in ball models it can be seen that dislocations cause a bending of the lattice in their immediate neighbourhood so that coherent X-ray reflection will not occur over regions much greater than the dislocation separation. The study of specific heat, plasticity, and magnetic properties suggests that cold working increases the dislocation density to a limiting value of approximately $10^{12}$ lines per $cm^2$ in the fully cold worked state. For a random distribution of dislocations these figures correspond to average distances between neighbouring dislocation lines of $10^{-6}$ cm. for the cold worked state, values which are in good agreement with those reported by Wood [21]. Each dislocation is surrounded by a slowly varying strain field, and thus a material containing dislocations will show both strain broadening and particle size broadening, the greater the density of dislocations, the greater in general being the broadening due to both causes. Annealed metals may be expected to show some strain broadening as observed (since they are generally assumed to contain of the order of $10^8$ dislocations per $cm^2$), although this is

very small and must have passed unnoticed in most experiments.

The actual value of the breadths from the cold worked metal will be very much influenced by recovery, which has been discussed by Koehler [38], Burgers [34], Cahn [39] and Guinier and Tenevin [40]. Although the mechanism of recovery is not fully understood it seems certain that it involves the migration of the dislocations into walls, similar to grain boundaries. It has been shown that such a mechanism can reduce the strain energy of the lattice. Recovery is thus dependent on the mobility of the dislocations and is greater for soft metals than for hard ones, and can be reduced by the presence of impurities (e.g. Cottrell and Churchman [41], and Bilby [42]). Thus the differences in strain found by Hall when interpreting previous results may be due either to the production of different dislocation densities by different method of working, or to different degrees of recovery, but in the present results they are due entirely to recovery.

In addition to the reduction in strain energy on recovery, reduction in particle size broadening is to be expected since reflection will be coherent over distances of the same order as the separation of polygonised boundaries. The small change observed in aluminium suggests that extensive polygonisation had occurred in the commercial purity specimen.

Thus the results from aluminium would agree with the predictions of the dislocation theory, the commercial purity aluminium having a higher strain energy (as indicated by the breadths) than the high purity aluminium because of the action of the impurities in restricting the movement of the dislocations. Any alternative theory of the changes would have to be based on a different type of metastable fault and would thus not be significantly different.

## Line Broadening Results from Wolfram

The measured line breadths from the spectra from the three samples of wolfram are shown in Figure 6. The increase in the breadths from the annealed sample at high angles is very marked, partly because of the reduced experimental breadth in this particular series of experiments and partly because wolfram line 16 occurs at a higher angle than aluminium line 24. Thus the existence of a definite physical broadening in the annealed metal is more apparent than in the study of aluminium, though a subsidiary experiment on an annealed aluminium specimen showed that the breadth of line 24 coincided
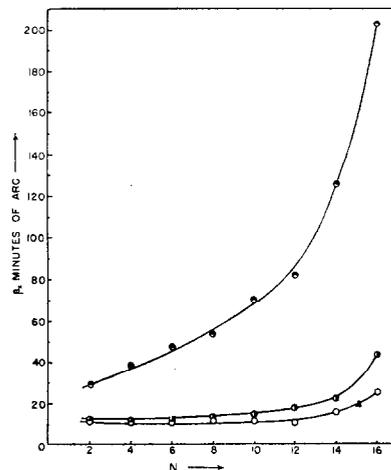


FIGURE 6. The line breadths $\beta_\chi$ for the wolfram spectra plotted against $N$. O from the sample annealed at 1300°C; ◖ from the sample recovered at 1150°C; ◕ from the sample examined as filed; ▲ subsidiary measurement of aluminium line 24.

with the curve through the breadths from the annealed wolfram.

The breadths from the specimen heated at 1150°C are only slightly greater than those from the annealed specimen and indicate that very extensive recovery has taken place from the high values of the breadths given by the cold worked specimen. Measurements of the background level showed that both the cold worked specimen and that heated at 1150°C gave similar background levels, which were significantly higher than that from the specimen annealed at 1300°C, indicating that the former had recovered and the latter had recrystallised.

A plot of $\beta^*$ against $d^*$ is shown in Figure 7, using a similar method of analysis to that used for aluminium. The analysis has been carried out for the recovered and annealed samples by assuming a constant breadth of 10 minutes of arc for line 2 and for a point midway between lines 14 and 16, posi-
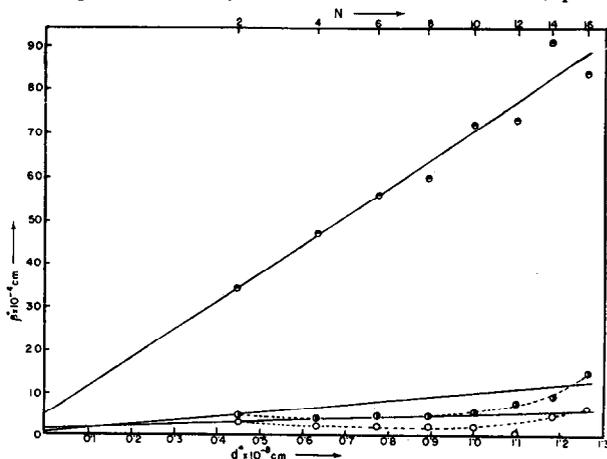


FIGURE 7. The interpretation of the line broadening in the wolfram spectra. Symbols as in Figure 6.

tions which are approximately equidistant from $\chi = 90°$. The plot which represents the annealed sample then has an intercept corresponding to $10^{-4}$ cm. and a small slope corresponding to a strain breadth 0.03 per cent. The intercept for the recovered metal indicates a similar particle size to that in the annealed state and a greater apparent strain having a value of approximately 0.1 per cent. This result suggests that if the postulated mechanism of recovery is correct, the separation of the walls of dislocations in the recovered state in this particular specimen is of the same order of magnitude as the separation of dislocations in the annealed state. The cold worked sample shows much greater particle size broadening, indicating a particle size of the order of $2 \times 10^{-5}$ cm, and a much greater value of the strain breadth of 0.62 per cent.

Thus the results from wolfram support the dislocation theory of deformation as closely as do those from aluminium, the only appreciable difference in the two sets of results being the greater strain and particle size broadening of the cold worked wolfram. The observed fractional rises in the background intensity from the two metals coincide fairly closely and indicate that the dislocation densities in both cold worked specimens are approximately equal. However, since the observed strains in the two metals differ so greatly, it is apparent that appreciable recovery must have occurred even in the commercially pure aluminium specimen. Such an interpretation is reasonable since the mobility of dislocations is a function of both the impurity content and the atomic mobility, which will in turn be a function of the melting point. Thus dislocations in the aluminium (melting point 933°A) will be more mobile at the temperature produced during filing ($\sim 600°$A) than in wolfram (melting point approximately 3700°A).

## Fourier Analysis of the Line Shapes

Interpretation of the Fourier coefficients has been carried out by the method of Warren and Averbach [17]. This method is unsuitable for determining particle sizes as large as $10^{-5}$ cm. occurring simultaneously with strain since errors in the analysis due to numerical summation and slight errors in placing the peak of the line reduce the reliable accuracy of the coefficients to three figures, leaving the value of particle size indeterminate.

An interesting feature of the plots of $A_n$ versus $n$ shown in Figure 8 for aluminium is that the values of $A_n$ from line 24 do not decrease as rapidly as do those from line 4, at low values of $n$. Since the coefficients
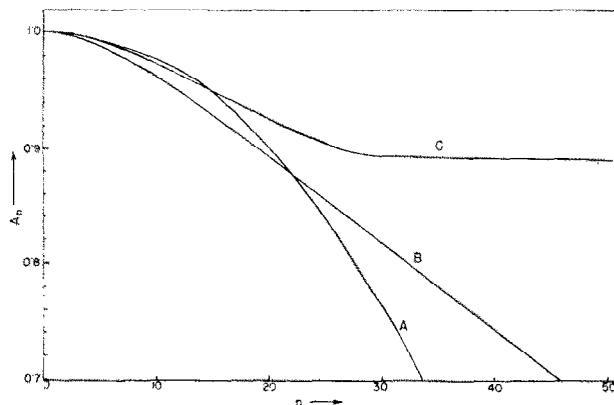


FIGURE 8. The Fourier coefficients of the broadening functions of some lines in the aluminium spectra. The curves have been drawn through the experimental points obtained at values of $n = 0, 1, 2, 3, 4, 5, 10, 30, 40$, and $50$. A for line 24, B for line 4, from the filed commercially pure sample; C for line 4 from the filed high purity sample.

are given by the $\langle \cos 2\pi l Z_n \rangle_{av.}$ where $Z_n$ is the displacement between two points $n$ cells apart they should decrease more rapidly for line 24, than for line 4. This apparent anomaly can be readily explained if it is assumed that the annealed specimen produces broadened lines, particularly at high Bragg angles.

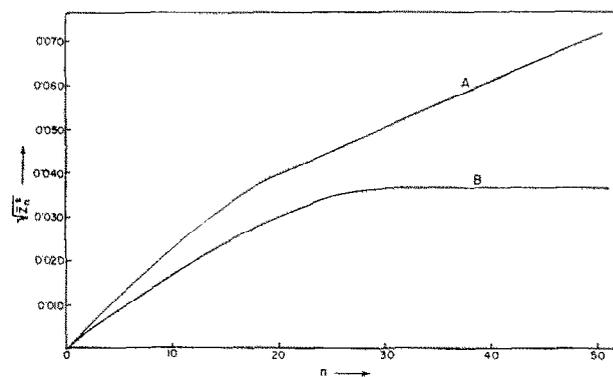The values of $\sqrt{\bar{Z}_n^2}$ for line 4 from the two purities of aluminium are plotted in Figure 9. The



FIGURE 9. The variation of $\sqrt{\bar{Z}_n^2}$ with $n$ for line 4 aluminium. The curves have been fitted to experimental points at the same values of $n$ as in Figure 8. A for the commercially pure sample; B from the high purity sample.

curve for the commercially pure specimen has the form previously reported by Warren and Averbach for $\alpha$-brass which they interpret as showing that the strains are not constant over regions of greater than about 10 spacings. The plot for the high purity specimen however is unusual in that the value of $\sqrt{\bar{Z}_n^2}$ becomes constant above values of $n = 30$. Similar results, shown in Figure 10 have been obtained from wolfram. This result is surprising because a truly random arrangement of strains would result in a curve continuing to rise smoothly towards a
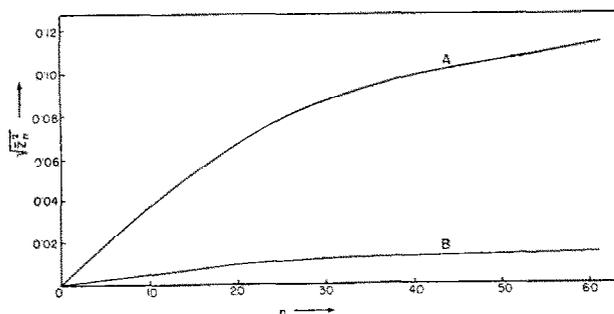
FIGURE 10. The variation of $\sqrt{\bar{Z}_n{}^2}$ with $n$ for line 14 wolfram. The curves have been fitted to the experimental points at the same values of $n$ as in Figure 8. A from the as filed sample; B from the sample recovered at 1150°C.

value of $\frac{1}{2}$ and thus the strains must take up some regular arrangement. This constancy implies that, to a good approximation, the regions of strain cannot extend for distances greater than 30 spacings. If this were not so the values of $\sqrt{\bar{Z}_n{}^2}$ would continue to increase beyond $n = 30$. If dislocations are accepted as causing the diffraction effects studied then this process would correspond to polygonization, and the walls of strain would bound the regions of coherent reflection. Thus the condition of the recovered specimen may be represented schematically as in Figure 11, in which walls of strain occur
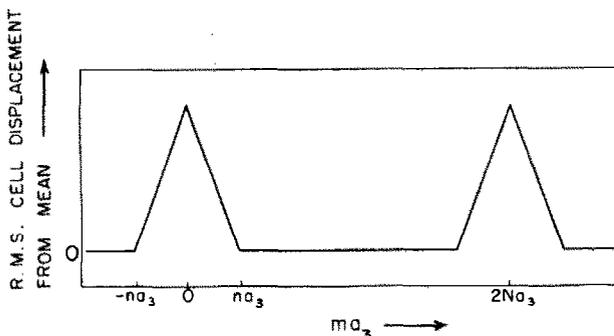


FIGURE 11. Schematic representation of the variation of the root mean square displacement of the cells with distance in recovered metals.

$2N$ spacings apart, and $2m$ spacings wide. To calculate the average absolute or mean square strains for all pairs of cells $n$ spacings apart, three terms must be considered:

(a) the displacement between cells in the wall, for values of $n < m$, $(m - n)$ cells exist having a displacement $Z_n \sim n\epsilon$ where $\epsilon$ is the strain in the wall, and for values of $n > m$ the contribution of this term is zero.

(b) the displacement between cells, one of which is in the strain free region and the other in the strained region. For values of $n < m$, $(n - 1)$ such combinations exist for each wall and have values $\epsilon, 2\epsilon, 3\epsilon, \ldots, (n - 1)\epsilon$, whereas for values of $n > m$

$(m - 1)$ such combinations exist having values $\epsilon, 2\epsilon, 3\epsilon, \ldots, (m - 1)\epsilon$.

(c) the additional displacement if slight strains occur in the so-called strain free region.
Neglecting the contribution from (c) the mean strain for $n < m$ is given approximately by:

$$(16) \quad \sqrt{\bar{Z}_n{}^2} \sim \bar{Z}_n = \frac{(m - n)(n\epsilon) + \sum\limits_{j=0}^{j=n} (j - 1)\epsilon}{N}$$

and for $n > m$,

$$(17) \quad \bar{Z}_n = \frac{0 + \sum\limits_{j=0}^{j=m} (j - 1)\epsilon}{N} = \text{constant.}$$

Thus $\bar{Z}_n$ gradually increases until at a value $n = m$ it becomes a constant. The width of the walls is thus about 30 atoms in both the aluminium and the wolfram. This analysis confirms the postulated mechanism of recovery, that the dislocations migrate into walls surrounding relatively large strain free regions. The analysis, however, throws some doubt on the usual interpretation of the $A_n$ versus $n$ plots, that the strains are non-uniform over distances greater than 10 spacings; a possibly more correct interpretation is that in certain regions the strains change appreciably over the distance of 10 spacings.

The surprising feature of the plots from the cold worked samples is their general similarity, despite the large recovery of the commercially pure aluminium, and it appears that this method of analysis is not sensitive to recovery until the recovery is almost complete.

## Conclusions

The changes in line profile with cold work have been correlated with the changes in intensity and it is shown that some lattice defects such as dislocations must be present in the cold worked state. The presence of broadening in the spectra of the annealed metals indicates that a smaller density of dislocations persists even after annealing. The differences in the apparent strains between the aluminium and wolfram spectra may be interpreted entirely in terms of the instantaneous recovery without necessitating either a different mechanism or dislocation density. Fourier analysis of the line shapes, confirms the above interpretations and indicates that the postulated mechanisms of recovery, namely, the migration of the dislocation into walls, is correct, at least for the later stages of recovery.

The above interpretation, however, is basically dependent on the observed changes in background

level measured in the spectra of aluminium and wolfram, and although the theory is expected to apply generally the lack of experimental evidence as to the nature of the intensity changes in the spectra of other materials makes this uncertain.

## Acknowledgements

## References

1. HALL, W. H. and WILLIAMSON, G. K. Proc. Phys. Soc. 64B (1951) 937, 946.
2. STOKES, A. R. and WILSON, A. J. C. Proc. Camb. Phil. Soc., 40 (1944) 197; Proc. Phys. Soc., 56 (1944) 174.
3. LIPSON, H. Symposium on Internal Stresses in Metals and Alloys (London, Institute of Metals, 1948), 35.
4. JONES, F. W. Proc. Roy. Soc., A166 (1938) 16.
5. SCHULL, C. O. Phys. Rev., 70 (1946) 697.
6. STOKES, A. R. Proc. Phys. Soc., 61 (1948) 382.
7. VAN ARKEL, E. A. Physica, 5 (1925) 208.
8. WOOD, W. A. Phil. Mag., 14 (1932) 636.
9. WOOD, W. A. Phil. Mag., 19 (1935) 219.
10. HAWORTH, F. E. Phys. Rev., 52 (1937) 613.
11. BRINDLEY, G. W. and RIDLEY, P. Proc. Phys. Soc., 50 (1939) 432, 501.
12. BRINDLEY, G. W. Proc. Phys. Soc., 52 (1940) 117.
13. SMITH, C. S. and STICKLEY, E. E. Phys. Rev., 64 (1943) 191.
14. STOKES, A. R., PASCOE, K. J., and LIPSON, H. Nature (London), 151 (1943) 137.

15. MEGAW, H. D. and STOKES, A. R. J. Inst. Met., 71 (1945) 279.
16. AVERBACH, B. L. and WARREN, B. E. J. Appl. Phys., 20 (1949) 885.
17. WARREN, B. E. and AVERBACH, B. L. J. Appl. Phys., 21 (1950) 595.
18. DEHLINGER, U. and KOCHENDÖRFER, A. Z. Metallkunde, 31 (1939) 231.
19. BRAGG, W. L. Nature (London), 149 (1942) 511.
20. BRAGG, W. L. Proc. Camb. Phil. Soc., 45 (1949) 125.
21. WOOD, W. A. Proc. Roy. Soc., A172 (1939) 231.
22. WOOD, W. A. Nature (London), 151 (1943) 558.
23. WOOD, W. A. and RACHINGER, W. A. J. Inst. Met., 75 (1949) 571.
24. STOKES, A. R. and LIPSON, H. Nature (London), 163 (1949) 871.
25. HALL, W. H. Proc. Phys. Soc., A62 (1949) 741.
26. WILSON, A. J. C. Acta Cryst., 2 (1949) 220.
27. MAZUR, J. Nature (London), 164 (1949) 358.
28. KRAINER, H. Arch. Eisenhuttenw., 22 (1951) 53.
29. WAINWRIGHT, C. Brit. J. Appl. Phys., 2 (1951) 157.
30. HALL, W. H. and WILLIAMSON, G. K. J. Sci. Inst., 29 (1952) 132.
31. RACHINGER, W. A. J. Sci. Inst., 25 (1948) 254.
32. ALEXANDER, L. J. Appl. Phys., 21 (1950) 126.
33. HIRSCH, P. B. and KELLAR, J. N. Proc. Phys. Soc., 64B (1951) 369.
34. BURGERS, W. G. Proc. Roy. Acad. Sci. Amsterdam, 50 (1947) 452.
35. COTTRELL, A. H. Progress in Metal Physics, 1 (1949) 77.
36. BRAGG, W. L. and NYE, J. F. Proc. Roy. Soc. A190 (1947) 474.
37. BILBY, B. A. J. Inst. Met., 76 (1950) 613.
38. KOEHLER, J. S. Phys. Rev., 60 (1941) 397.
39. CAHN, R. W. Progress in Metal Physics, 2 (1951) 151.
40. GUINIER, A. and TENEVIN, J. Progress in Metal Physics, 2 (1951) 177.
41. COTTRELL, A. H. and CHURCHMAN, A. T. J. Iron and Steel Inst., 162 (1949) 271.
42. BILBY, B. A. Proc. Phys. Soc., A63 (1950) 191.